PECULIARITIES OF CORROSION AND ELECTROCHEMICAL BEHAVIOR OF SUPERELASTIC Ti-Nb-BASED ALLOYS FOR BIOMEDICAL APPLICATION

Zhukova Yu.S., Konopatsky A.S., Pustov Yu.A., Filonov M.R., Prokoshkin S.D., Brailovski V.

National University of Science and Technology "MISiS", 119049 Moscow, Russia

zhukova@misis.ru

Shape memory and superelastic Ti-Nb-based alloys with the Ta and Zr addition are considered as advanced biomedical materials for intraosseous implants. They exhibit high biocompatibility due to absence of harmful elements and high biomechanical compatibility with bone tissues due to low Young's modulus and superelastic behavior based on reversible $\beta \leftrightarrow \alpha''$ martensitic transformation [1,2]. A load-bearing implant is always subjected to cyclic loads up to 1% strain during its life cycle. However, the information about Ti-Nb-based alloys superelastic fatigue behavior in simulated physiological media is lacking.

The aim of the present work was to study electrochemical behavior of superelastic Ti-Nb-Ta and Ti-Nb-Zr alloys under cyclic loads up to 1.5 % strain.

The experimental samples were the wires of Ti-19.7Nb-5.8Ta (TNT) and Ti-21.8Nb-6Zr (TNZ) (at. %) alloys in recrystallized condition after hot forging for TNT and hydrostatic pressing for TNZ followed by water-quenching from 900 °C. The experimental procedure included open circuit potential (OCP) measurements in Hank's solution simulating inorganic components of bone tissue at 37 °C. Saturated silver / silver chloride electrode (hereafter SSCE) was used as reference electrode. Cyclic loads up to 0.2, 0.4, ...1.5 % strain were applied to the samples using the experimental setup shown in Fig. 1 [3].

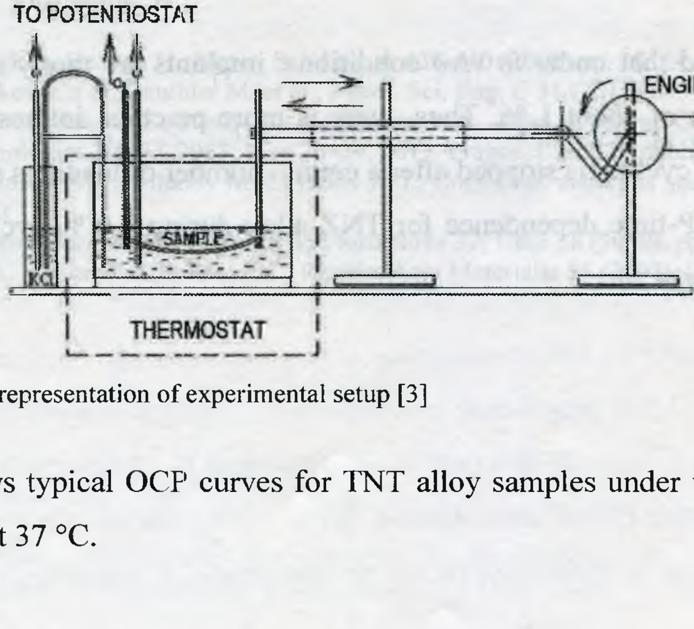

Figure 1. Schematic representation of experimental setup [3]

Fig. 2 shows typical OCP curves for TNT alloy samples under various cyclic loads in Hank's solution at 37 °C.

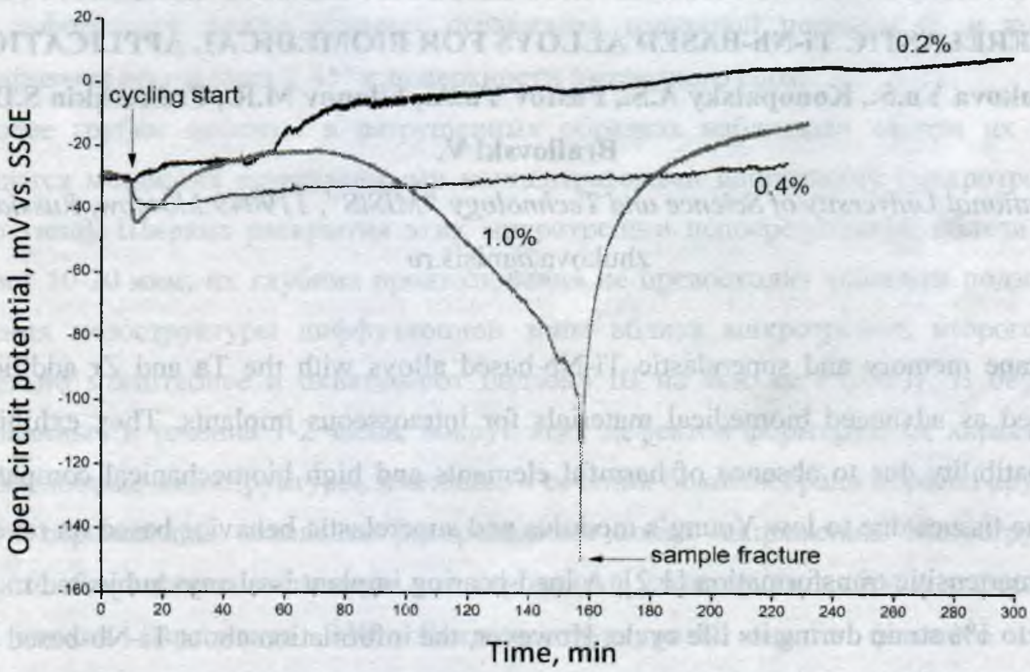

Figure 2. OCP curves of TNT alloy under cyclic loads with various strain values

Significant OCP drops can be observed at the moment of the cycling start indicating the passive oxide film breakdown. The amplitude of this drop increases at higher strain values.

The following OCP rise (Fig. 2, curve "0.2%") can be explained by chemomechanical effect resulting in oxide film plastification, which was previously observed for pure titanium [4]. The strain increase leads to destabilization of the passive film which resists OCP positive shift (Fig. 2, curve "0.4%"). At higher strain values (Fig. 2, curve "1.0 %") one can observe OCP curve with extremum (maximum). The ascending part of the curve can be explained by intensive chemomechanical effect while the smoothly descending part is caused by the fatigue crack propagation inhibited by stress-induced formation of martensite crystals near the crack tip [5,6].

It should be noted that under *in vivo* conditions, implants are rarely subjected to high (even short-time) strain of about 1 %. Thus, there is more practical interest in studying the cases when mechanical cycling is stopped after a certain number of loadings and unloading.

Fig. 3 shows OCP-time dependence for TNZ alloy during 1.0 % cycling and after its stop at different test stages.

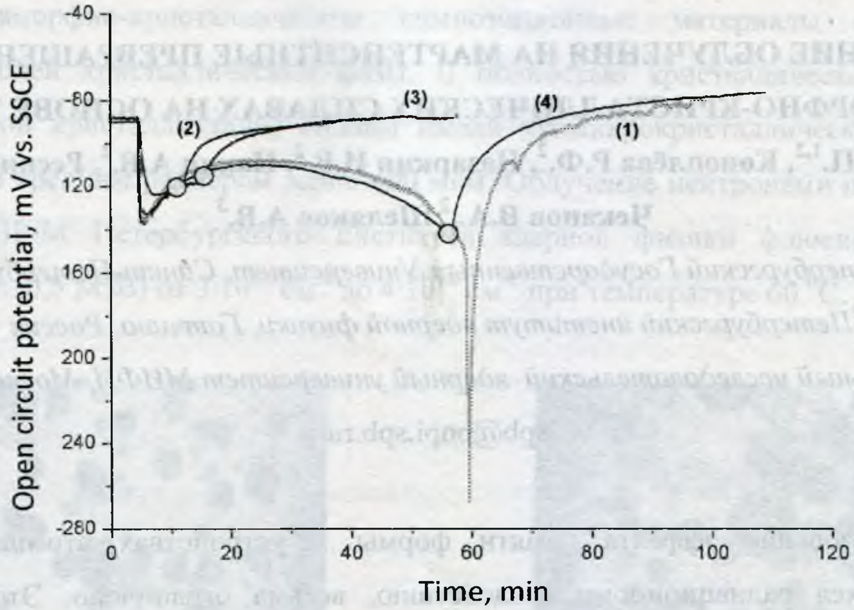

Figure 3. OCP curves of TNZ alloy uring continuous mechanocycling with 1.0 % strain (curve 1) and with cycling stop at different test stages (curves 2, 3, 4). Circles on the curves indicate the moment of cycling stop

It can be seen from Fig. 3 that regardless the OCP value at which the cycling was stopped, the specimen exposure is accompanied by potential increase up to the values close or slightly higher than those before cycling.

Conclusions

Open circuit potential measurements of superelastic Ti-19.7Nb-5.8Ta and Ti-21.8Nb-6Zr alloys were carried out in Hank's solution with various strain values up to 1.5 %. At moderate strain values of about 0.2 %, the alloys tend to plastificate and effectively resist to corrosion fatigue under stress. At much higher strains (about 1 %), the martensite formation is presumably responsible for the increase in fracture toughness and inhibiting fatigue crack propagation.

1. Miyazaki S., Kim H.Y., Hosoda H., Mater. Sci. Eng. A 438-440 (2006) pp. 18–24.
2. Brailovski V., Prokoshkin S., Gauthier M. et al., Mater. Sci. Eng. C 31 (2011) 643–657.
3. Zhukova Yu.S., Konopatsky A.S., Pustov Yu.A., Filonov M.R., Proc. of the Int. Conf. on Shape Memory and Superelastic Technologies, SMST 2013, May 20–24, 2013, Prague, Czech Republic, p. 374-375.
4. Pustov Yu.A., Kutuzov A.V., Filonov M.R., Belov M.I., Corrosion: materials and protection 10 (2011), pp. 12-21. [in Russian]
5. Yi S., Gao S., International Journal of Solids and Structures 37, Issue 38 (2000), pp. 5315–5327.
6. S.W. Robertson, A. Mehta, A.R. Pelton, R.O. Ritchie, Acta Materialia 55 (2007), Is. 18, p. 6198–6207.